Limit Analysis for Porous Materials in Plane Strain

Fabio da Costa Figueiredo, ffigueiredo@mecsol.ufrj.br
CEFET-RJ, Departamento de Engenharia Mecânica - Av.Maracanã, 229 - Rio de Janeiro, RJ, Brazil
UFRJ-COPPE, Programa de Engenharia Mecânica - Av. Brigadeiro Trompowski,s/n, Centro de Tecnologia, bloco G - Rio de Janeiro, RJ, Brazil

Lavínia Borges, lavinia@ufrj.br
UFRJ-COPPE, Programa de Engenharia Mecanica - Av. Brigadeiro Trompowski,s/n, Centro de Tecnologia, bloco G - Rio de Janeiro, RJ, Brazil

Abstract. *On plasticity theory two methods are widely used to solve structural analysis problems: the incremental method and direct method. Unlike incremental method, in direct method there is no need to analyze the structure behavior during each load step in order to compute critical states and collapse mechanisms. The shakedown and limit analysis are the main representatives of the direct methods. In this paper, from maximum plastic dissipation principle and the set of admissible stress fields, a limit analysis formulation for porous materials is proposed.In order to model a problem in plasticity, the choice of an appropriate yielding function is mandatory. For ductile materials, the stress deviatory dependent von Mises criterion is largely used. However for porous materials, like soils, ceramic materials and powder metals, the von Mises criteria does not consider the main variables that describes his mechanical behavior such as friction angle, cohesion and the porosity. Moreover, those materials are pressure dependents and the stress invariant* I_1 *must be taken into account. Thus, a* J_2 *and* I_1 *dependent yield function is proposed and it takes into account all the described porous materials properties. Depending on these properties, a critical porosity is calculated and the yield function may assume an elliptical or an hyperbolic shape.The problem of interest is a plane strain and applying the normality rule, one normal strain component is made null and the stress in that direction is derived, function of others components. This kind of problem is applied to describe among others, indentation problems and scratch tests on porous materials. In indentation tests, a rigid indenter is punched against the tested material. In scratching tests, an indenter made of rigid material is dragged on the material tested surface. Controlled forces are applied and the penetration depth remains constant. Both tests are realized on nanoscale and the main objectives of them is to get the hardness of porous materials.*

Keywords: *limit analysis, porous materials, strain plane.*

1. INTRODUCTION

In oil industry, due the necessity of extracting oil from deep waters, subsea pipes are submitted to severe mechanical efforts. In deep waters, pipes are submitted to high external pressure and eventually to high temperatures and since the pipe is not free, i.e., there are supports and anchors restraining movements, compressive forces are developed due to water column pressure and pipe thermal expansion. Under these conditions, compressive stresses may reach a critical magnitude and buckling may occur, leading to a catastrophic failure and causing structure collapse. On the other hand, buckling is not a problem if it is controlled and induced on pipes in order to relief high stresses.

Buckling occurrence, among many variables, depends on friction between pipe-soil and this interaction must be understood. In pipe buckling two situations may occur: the pipe can get out from the trench or it can drag the amount of soil around his vicinity. To model this problem, the pipe is described as a rigid structure dragging a soft material (soil). This may be idealized as a scratch test problem, where a rigid indenter is dragged into a material. The indentation problem, where a indenter is pressed against a surface is also studied. Both problems are solved using plasticity theory and limit analysis method by an algorithm developed by Borges (1991). Limit analysis is a direct method and there is no need to analyze the structure behavior during each load step. The results required are the collapse factor α, the stress and velocity fields and the plastic multiplier λ.

Modeling the mechanical behavior of porous materials is a difficult task since many variables are involved. The development of plasticity studies on porous materials have wide applications like material hardness determination using nondestructive methods by indentation or scratch tests. Porous materials comprise soils (sand, clay), ceramics or even metallic powder, where the metal is physically divided into many small particles, then passing through compression and sintering processes. Indentation tests are very useful in civil engineering and geotechnics in piling problems. As another application of indentation problems, Cariou (2006) by means of nanoindentation techniques identifies mechanical properties in cohesive-frictional porous materials. Due to heterogeneity of sedimentary rocks, the application of nanoindentation has provided a new versatile tool to test in situ phase and structures of geomaterials that cannot be recapitulated ex situ in bulk form. This technique requires a rigorous indentation analysis to translate indentation data into meaningful mechanical properties. The application of this technique is also made by Sorelli *et al.* (2008). Similarly to indentation tests, scratch tests are also used as an alternative way of measuring mechanical properties as adhesion of coatings or strength of rocks, according to Bard and Ulm (2009). This kind of test consists in dragging a rigid indenter onto the tested material, at constant depth and controlled forces.

In this work, based on limit analysis formulation, indentation and scratch test problems are discretized in a 2-D finite elements method. Moreover, an appropriate yield function must be chosen to include the material porosity effects, soil cohesion and friction angle. The influence of stress invariant I_1 (mean stress) is also observed. The use of Mori-Tanaka morphology is then applied and it includes such cited variables. In this morphology, according to a critical porosity, the yield function may be either elliptical or hyperbolic. Under such special conditions, this function becomes asymptotically to a Drucker-Prager or von Mises criterion. More details about this subject are in Gathier (2006). Plane deformation hypothesis is applied and the yield function is derived concerning this hypothesis. Hereafter, this plane deformation formulation is implemented in the computational model, developed in Fortran®. Then the scratch test and indentation collapse factors are plotted and compared to analytical solutions.

2. Model

This section shows schematically the geometry of indentation and the scratch test problems. Some comments on porous materials are also made as well as limit analysis method and the discretization scheme. Then, an yield function in plane is developed and implemented in the computational model.

2.1 Geometry

Figure 1 shows schematically the geometry of indentation problem. As observed, a rigid indenter is pressed against a material surface. This indenter may have different shapes like spherical, conical and pyramidal, with many opening angles as found in Cariou (2006).

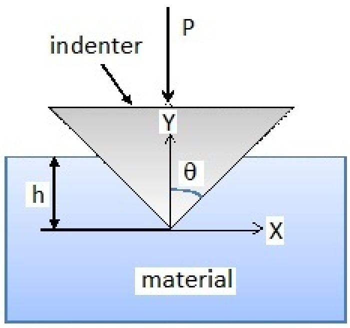

Figure 1. Schematic of an indentation test.

Figure 2 shows schematically the scratch test geometry. In this test, an indenter of certain opening angle θ is dragged into the material at a constant depth d. Conveniently, in order to calculate an analytical solution, the material is partitioned in three zones with constant stresses fields, defined by the angle β.

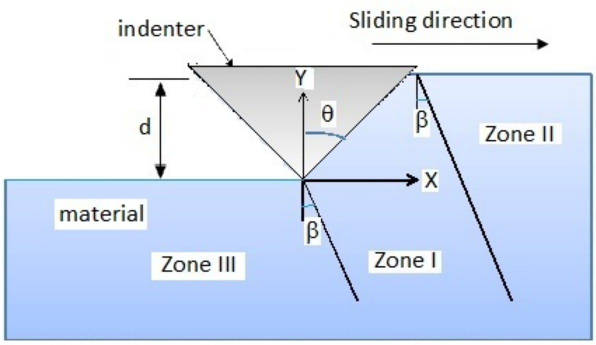

Figure 2. Schematic of a scratch test.

In both problems it is not taken into account the material accumulation that is generally formed on vicinity of contact area of indenter on the indentation problem and in front of indenter for the scratch test.

2.2 Discretization Scheme

The continuum form of the limit analysis problem is discretized into 2-D mixed finite elements, applied to solve both indentation and scratch problems. Triangular elements are used, with quadratic interpolation for velocity and linear interpolation for stresses fields. An adaptive mesh refinement is used and the goal of this approach is to achieve a mesh-adaptive strategy accounting for mesh size refinement, as well as redefinition of the element stretching. More details about adaptive approach are in Borges *et al.* (2001). The algorithm developed by Borges (1991) allows the choice of mesh refinement level. The refinement level 0 mesh implies an uniform mesh. After that, the adaptive mesh is applied on interest area of the problem, leaving a coarse mesh on unimportant areas.

2.3 Limit Analysis Model

Limit analysis method aims the determination of the loads that will cause the phenomenon of incipient plastic collapse, in a body made of elastic ideally plastic material. This method have been widely studied by many researchers and see Borges (1991), Zouain *et al.* (1993) and Pontes *et al.* (1997) for more information. The extremum principles for limit analysis of continuum bodies under proportional loads are presented hereafter.

Consider a body that occupies a region $\mathcal{B}$ with regular boundary Γ and let V the function space of all admissible velocity fields *v* complying with homogeneous boundary conditions prescribed on Γ_u of Γ. The strain rate tensor denoted by D relates with *v* by a linear operator and the duality product between stress fields T and strain rate D belonging respectively from spaces $W^{'}$ and W is written as:

$$\langle T, D \rangle = \int_{\mathcal{B}} T.D \; d\mathcal{B} \tag{1}$$

The load system is represented by an element F from space $V^{'}$, dual of V. The duality product is denoted as:

$$\langle F, v \rangle = \int_{\mathcal{B}} b.v \; d\mathcal{B} + \int_{\Gamma_t} \tau.v \; d\Gamma \tag{2}$$

where *b* and τ are body and surface forces respectively, Γ_t is a part of boundary Γ where external loads are prescribed.

From equilibrium requirements:

$$\langle T, D \rangle = \langle F, v \rangle \tag{3}$$

The stress field *T* is constrained to fulfill the plastic admissibility condition, belonging to the set P defined as:

$$P = \{T \in W^{'} | f(T) \leq 0\} \tag{4}$$

The constitutive relations are derived from principle of maximum dissipation, associating the stress T and plastic dissipation $X(D^p)$ to a given strain rate D^p, as in Eq. (5):

$$X(D^p) = \sup_{T^* \in P} \langle T^*, D^p \rangle \tag{5}$$

Stress and plastic strain rates are related by an associative flow law and the complementary condition is also used, as seen in Lubliner (1990). Solving a problem using the limit analysis consists in finding a load factor α such the body undergoes to plastic collapse when subject to a reference load amplified by α. From classical extremum principles of limit analysis, the called static, kinematic and mixed formulations are derived and more information about these principles, limit analysis discretized forms and the algorithm that solves the optimization problem are found in Borges (1991), Zouain *et al.* (1993) and Pontes *et al.* (1997).

2.4 Porous materials

As is well known, soils are composed by a mix of lots of different particles, creating a very heterogeneous material. Because of its heterogeneity and presence of porous, the determination of mechanical properties of such materials becomes a difficult task. In order to solve this, the development of a predictive model for strength of porous materials will make extensive use of the theory of strength homogenization. Recent advances on homogenization techniques are found in Gathier (2006).

Porous materials with a dominating matrix-pore inclusion morphology are well represented by the Mori-Tanaka scheme, as seen in Gathier (2006) and Cariou (2006). In Mori-Tanaka scheme some material parameters such as $\alpha_d, \sigma_0, \alpha_m$ are calculated and they include the soil cohesion, porosity and friction angle effect. Once determined these parameters, the yield function is then determined. As an important remark, the yield function using this morphology may assume two distinct regimes, depending on density packing. Density packing is defined in Eq. (6):

$$\eta = \frac{V_s}{V_t} \tag{6}$$

where V_s is the solid volume and V_t is the material total volume, including pores.

In this morphology there is a density packing critical value, defining two yield function regimes: below this critical value the yield function assume an elliptic shape and over this value it assumes an hyperbolic shape. This critical density packing, denoted by η_{crit}, is a function of friction angle α_s and calculated as in Eq. (7):

$$\eta_{crit} = 1 - \frac{4\alpha_s^2}{3} \tag{7}$$

Under certain conditions, for example friction angle $\alpha_s = 0$ and packing density $\eta = 1$, the yield function becomes the von Mises criterion. And for $\alpha_s \neq 0$ and $\eta = 1$, the Drucker-Prager criteria is also asymptotically obtained. The graphic J_2 (deviatory) versus σ_m (mean stress) in Fig. 3 shows the yield function regimes:

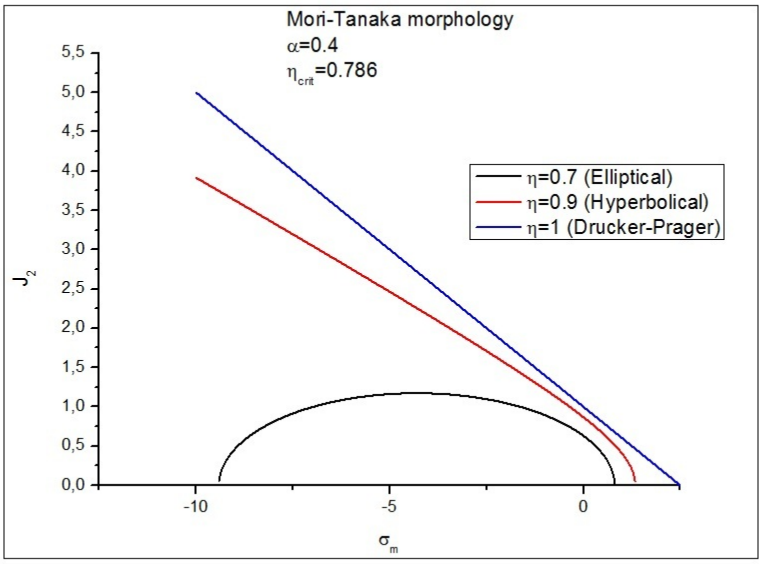

Figure 3. Yield function regimes: elliptical below η_{crit}, hyperbolical above this value and limited by Drucker-Prager when $\eta = 1$.

This graphic is plotted with friction angle $\alpha_s = 0.4$ fixed and the packing density critical value is obtained as a function of this angle, in this case one have $\eta_{crit} = 0.786$. It means that any packing density below this critical value the yield surface has an elliptical shape and otherwise, the criterion is hyperbolical. It is also observed that when $\eta \to 1$ the cone-shaped Drucker-Prager criterion is reached. If von Mises citerion were represented, it would be an horizontal line passing through $J_2 = 1$, parallel to mean stress axis since Mises is independent of the mean stress, as expected.

3. The Yielding Function in Plane Deformation

Equation (8) shows an elliptical yield function used in this work:

$$F(\mathbf{\Sigma_d}, \Sigma_m) = \left(\frac{\Sigma_m + \sigma_0}{\alpha_m}\right)^2 + \left(\frac{J_2}{\alpha_d}\right)^2 - 1 \tag{8}$$

where $\alpha_d, \sigma_0, \alpha_m$ are material parameters and calculated as seen in Gathier (2006) and Cariou (2006), $\mathbf{\Sigma_d}$ and Σ_m are deviatory and mean stresses respectively. Using projection operators, the deviatory is calculated as in Eq. (9):

$$\mathbf{\Sigma_d} = \mathbb{P}\,\mathbf{\Sigma} \tag{9}$$

where tensor $\mathbb{P}$ projects the stress vector Σ on deviatory space.

Letting the vector $\mathbf{m}$ representing the unitary vector along hydrostatic direction, the mean stress is calculated as in Eq. (10):

$$\Sigma_m = \frac{1}{\sqrt{3}}\mathbf{\Sigma}.\mathbf{m} \tag{10}$$

The decompositions of these stresses components are schematically presented in terms of principal stresses in Fig. 4, showing the hydrostatic axis $\mathbf{m}$ and the deviatory plane perpendicular to it:

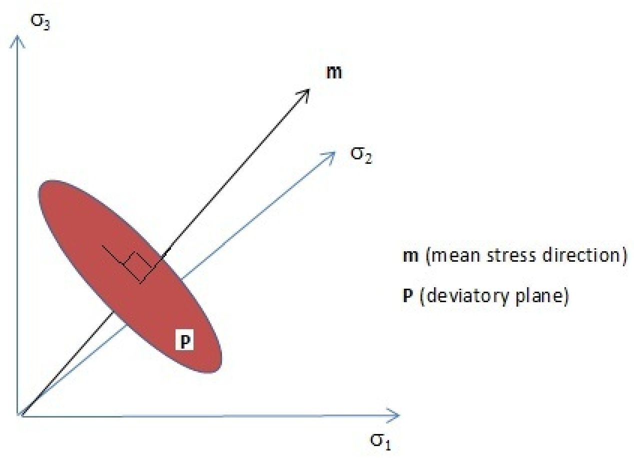

Figure 4. Hydrostatic axis and deviatory plane on principal stresses.

The invariant J_2 is defined in Eq. (11):

$$J_2 = \sqrt{\frac{1}{2}\mathbf{\Sigma_d}.\mathbf{\Sigma_d}} \tag{11}$$

From plane deformation hypothesis, the deformation component ϵ_z is made null. Applying the normality rule, then the stress component Σ_z is obtained in function of Σ_x and Σ_y components, as in Eq. (12):

$$\Sigma_z = \frac{\Sigma_x + \Sigma_y}{2}A - B \tag{12}$$

where: A=$\frac{\alpha_m^2 - 4\alpha_d^2}{2\alpha_d^2+\alpha_m^2}$ and B=$\frac{6\alpha_d^2\sigma_0}{2\alpha_d^2+\alpha_m^2}$.

In this way, a relation between a stress vector $\mathbf{\Sigma} = [\Sigma_x, \Sigma_y, \Sigma_z, \sqrt{2}\Sigma_{xy},]^T$ and the stress vector at plane deformation denoted by $\mathbf{\Sigma_p}$, with components $[\Sigma_x, \Sigma_y, \sqrt{2}\Sigma_{xy}]^T$ is made through Eq (14):

$$\mathbf{\Sigma} = \mathbb{P}_D\mathbf{\Sigma_p} + \mathbf{D} \tag{13}$$

where $\mathbf{D}$=$[0, 0, -B, 0]^T$ and $\mathbb{P}_D$ is a 4x3 tensor, defined as follows:

$$P_D = \begin{bmatrix} 1 & 0 & 0 \\ 0 & 1 & 0 \\ A/2 & A/2 & 0 \\ 0 & 0 & 1 \end{bmatrix}$$

In an alternative way, the yield function described in Eq. (8) is rewritten as:

$$F(\mathbf{\Sigma}) = \frac{1}{2}\mathbb{C}\mathbf{\Sigma}.\mathbf{\Sigma} + a\,\mathbf{\Sigma}.\mathbf{m} - r_k \tag{14}$$

where $\mathbb{C} = \frac{1}{\alpha_d^2}\mathbb{P} + \frac{2}{3\alpha_m^2}(\mathbf{m} \otimes \mathbf{m})$, $a = \frac{2\sigma_0}{\sqrt{3}\alpha_m^2}$ and $r_k = 1 - \left(\frac{\sigma_0}{\alpha_m}\right)^2$

Rewriting this function using plane deformation formulation:

$$F(\mathbf{\Sigma_p}) = \frac{1}{2}\mathbb{C}_p \mathbf{\Sigma_p}.\mathbf{\Sigma_p} + \mathbf{P_k}.\mathbf{\Sigma_p} + R_k \tag{15}$$

where:

$$\mathbb{C}_p = \mathbb{P}_D^T \, \mathbb{C}.\mathbb{P}_D \tag{16}$$

$$\mathbf{P_k} = \mathbb{P}_D^T \, \mathbb{C}.\mathbf{D} + a\mathbb{P}_D \, \mathbf{m} \tag{17}$$

$$R_k = \frac{1}{2}\mathbb{C} \, \mathbf{D}.\mathbf{D} + a\mathbf{D}.\mathbf{m} - r_k \tag{18}$$

Once defined the yield function on plane deformation, the Gradient and the Hessian of Eq. (15) are computed as:

$$\nabla_\Sigma F(\Sigma) = \mathbb{C}_p \, \mathbf{\Sigma_p} + \mathbf{P_k} \tag{19}$$

$$\nabla_\Sigma^2 F(\Sigma) = \mathbb{C}_p \tag{20}$$

Both gradient and hessian are used in the limit analysis algorithm and hessian shall be invertible.
Studying the eigenvalues and the eigenvectors of $\mathbb{C}_p$:

- Eigenvalues: $(\frac{1}{\alpha_d^2}, \frac{1}{\alpha_d^2}, \frac{12\alpha_d^2+\alpha_m^2}{(2\alpha_d^2+\alpha_m^2)^2})$
- Eigenvectors: $[0,0,1]^T, [-1,1,0]^T, [1,1,0]^T$

Decomposing $\mathbb{C}_p$ using spectral theorem, the characteristic spaces are the deviatory plane, defined by eigenvectors $[0,0,1]^T$ and $[-1,1,0]^T$ and the hydrostatic axis, defined by eigenvector $[1,1,0]^T$. Thus, every vector on deviatory plane is an eigenvector of $\mathbb{C}_p$. Moreover, the positive-definiteness of $\mathbb{C}_p$ is proved since the properties α_d and α_m are positive (only on elliptical case) and consequently, the eigenvalues are always positive also.

4. Results

In this section results for the scratch test and indentation problems are compared to a semi-analytical lower bound solution. The scratch test semi-analytical solution seen in Bard and Ulm (2011) is used considering Mori-Tanaka morphology and it was implemented in MathCad®. Then, these results were compared to discretized Limit Analysis.

The collapse factors α from both aproaches were compared, choosing some friction angles values and making the packing density η to vary. Figures 5 and 6 compare the collapse factors, where the continuous line represents the ones obtained by analytical solution, calculated by lower limit bound solution.

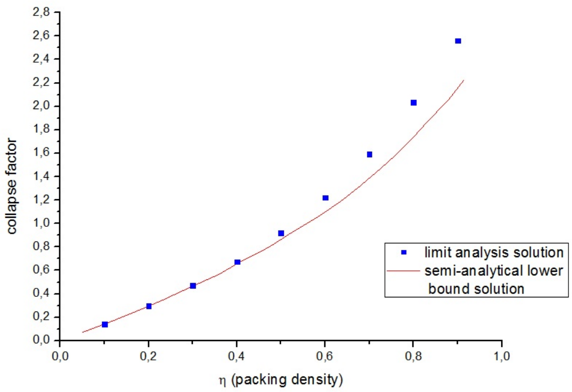

Figure 5. Results for $\alpha_s = 0.1$.

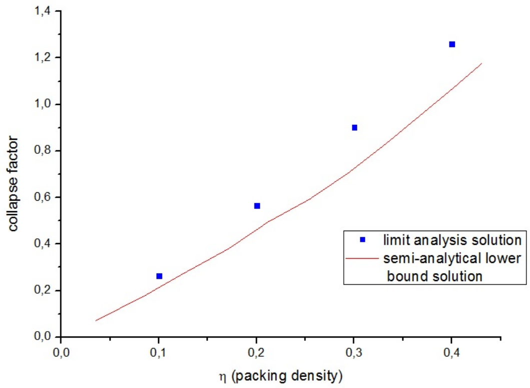

Figure 6. Results for $\alpha_s = 0.5$.

Both graphics correspond to density packing lower than the critical value η_{crit}, ie, the yield function has the elliptical shape. Figures 7 show the adaptive mesh used before running the limit analysis algorithm. One may observe that, using an adaptive mesh there is a fine mesh on the vicinity of the indenter and a coarse mesh out of this interest area. After converging the limit analysis algorithm, Fig. 8 shows the plastic multiplier distribution, after running an example with $\alpha_s = 0.1$ and $\eta = 0.9$.

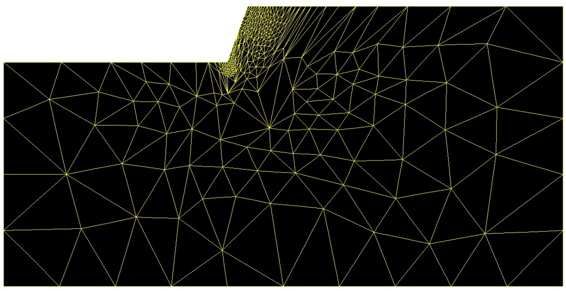

Figure 7. Scratch test mesh for $\alpha_s = 0.1$.

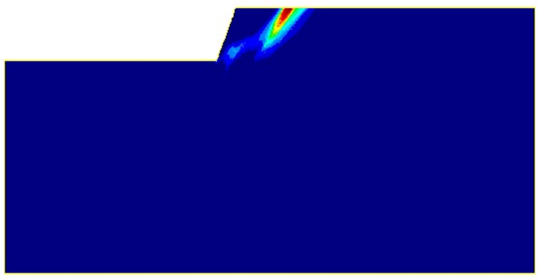

Figure 8. Plastic multiplier distribution for $\alpha_s = 0.1$ and $\eta = 0.9$.

For the indentation problem there is no an analytical solution considering the packing density influence and consequently the Mori-Tanaka morphology. However, there is a analytical solution considering slip lines theory and von Mises criterion in Lubliner (1990) and Kachanov (1971) and in this case the collapse factor is equal to $(2 + \pi)$, that is approximately 5.1415. It should be noted that from Eq. (8) and by making $\eta = 1$ and $\alpha_s = 0$, this elliptical yield function leads to von Mises criterion. An important issue in the indentation discretized limit analysis problem is the mesh dependent results. Both problems, scratch and indentation, are meshed by an adaptative process as described in Borges *et al.* (2001). Specifically on indentation problem, a better result is obtained as higher the adaptative mesh level is and the collapse factor gets even more closer to the analytical solution. With a refined mesh, the collapse factor reaches 5.166. Figures 9 and 10 show respectively the adaptive mesh used and the plastic multiplier distribution. Only half representation is made because of problem symmetric.

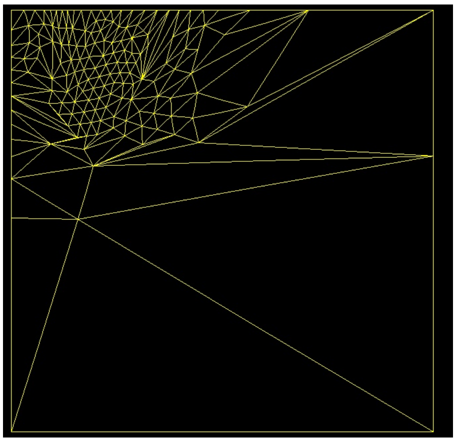

Figure 9. Mesh for the indentation test.

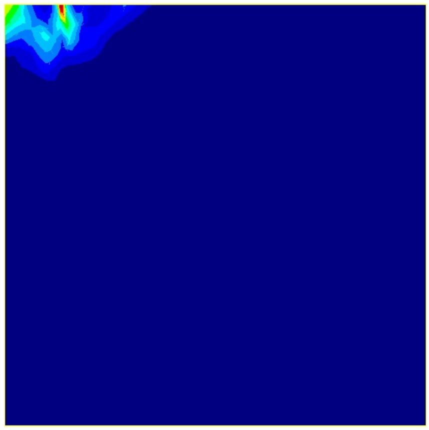

Figure 10. Plastic multiplier distribution from indentation test.

5. Results Discussion and Conclusions

Analysing the scratch test results, one can see that the results from discretized limit analysis using the mixed formulation are consistent with the semi-analytical solution. Since semi-analytical solution is a lower bound solution, the behavior of discretized limit analysis solution is as expected. On indentation problem, the result from limit analysis was close to the analytical solution and differing only in 0.47%.

In this paper it was shown a strain plane model developed to scratch an indentation tests problems. Using a mixed limit analysis method and an adaptive mesh discretization, the yield function was written in strain plane, as shown on previous sections. According to Mori-Tanaka morphology, the yield function may be elliptical or hyperbolical, depending on material packing density being below or above a certain critical value. The comparisons with analytical solutions are coherent and may validate the model. The problems studied were limited to elliptical yield function, since hyperbolic case brings on some development modeling difficulties and programming.

Since the results were well compared to analytical solutions, the next step is to develop the hyperbolical case, that will be applied to both problems. Then, the material accumulation influence formed around the indenter on indentation problem when it penetrates the material should be also considered in future work. On scratch test problem a 3-D stress model will be develop. This problem is specially important in order to study the interaction between a pipe and soil, subject to instabilities on seabed.

6. ACKNOWLEDGEMENTS

The author wants to thanks CNPq and CAPES for the financial support.

7. REFERENCES

Bard, R. and Ulm, F.J., 2009. "An analysis of scratch tests on porous cohesive-frictional material".

Bard, R. and Ulm, F.J., 2011. "Scratch hardness-strength solutions for cohesive-frictional materials". *International Journal for Numerical and Analytical Methods in Geomechanics*.

Borges, L., Zouain, N., Costa, C. and Feijóo, R., 2001. "An adaptative approach to limit analysis". *International Journal of Solids and Structures*, Vol. 38, pp. 1707–1720.

Borges, L.M.S.A., 1991. *Formulação e Solução para Análise Limite com Superfície de Escoamento Não Linear*. Ph.D. thesis, Pontificia Universidade Catolica, Rio de Janeiro.

Cariou, S., 2006. *The Effect of the Packing Density on the Indentation Hardness of cohesive-Frictional Porous Materials*. Ph.D. thesis, Massachussetts Institute of Technology, Massachussettsl.

Gathier, B., 2006. *Multi Scale Homogenization - Application to Shale Nanoindentation*. Ph.D. thesis, Massachussetts Institute of Technology, Massachussettsl.

Kachanov, L.M., 1971. *Foundations of the Teory of Plasticity*. North-Holland Publishing Company, Netherlands.

Lubliner, J., 1990. *Plasticity Theory*. Pearson Education, USA.

Pontes, I.D.S., Borges, L., Zouain, N. and Lopes, F., 1997. "An approach to limit analysis with cone-shaped yield surfaces". *International Journal for Numerical Methods in Engineering*, Vol. 40, pp. 4011–4032.

Sorelli, L., Constantinides, G., Ulm, F.J. and Toutlemonde, F., 2008. "The nano-mechanical signature of ultra high performance concrete by statistical nanoindentation techniques". *Cement and Concrete Research*, Vol. 38, p. 1447Ű1456.

Zouain, N., Herskovits, J., Borges, L. and Feijóo, R., 1993. "An interative algorithm for limit analysis with nonlinear yield functions". *International Journal of Solids and Structures*, Vol. 30, pp. 1397–1417.

8. Responsibility notice

The authors are the only responsible for the printed material included in this paper.